Flow and heat transfer characteristics of high temperature continuous rising bubbles

***Jiarui Xu*[a]，*Xiaohui Zhang*[a,*]，*Guangjun Zhang*[b]，*Shan Qing*[a]**

[a] Engineering Research Center of Metallurgical Energy Conservation and Emission Reduction, Ministry of Education, Kunming University of Science and Technology, Kunming 650093, China

[b] ENN Energy Holdings Limited, Langfang 065000, Hebei, China

[*] Corresponding author. E-mail address: xiaohui6064@qq.com

Abstract: In the movement process of continuous bubbles, different liquid flow state and initial temperature of bubbles have important influence on bubble movement and heat transfer. In this study, the flow and heat transfer characteristics of high temperature bubbles in normal temperature liquid are investigated. The rising process of and temperature of bubbles are studied by numerical simulation and compared with experimental results for verification. The results show that the shape, velocity and temperature of the bubble are affected by the initial position of the bubble. Because the closer the initial position of the bubble is to the bottom of the cylinder, the greater decrease of the bubble aspect ratio (w), the faster decrease of bubble temperature, and the larger bubble velocity would be. The increase of the bubble diameter would mitigate the influence of liquid jet on the bubble motion. Finally, as the bubble surface tension increases, the liquid jet would have less influence on the bubble movement.*

Key words: Continuous bubble; Two-phase flow; Flow characteristics; Heat transfer; Numerical simulation

1. Introduction

Bubble motion exists in many engineering processes, such as chemical engineering and metallurgy. It is of great significance to study bubble motion characteristics in industrial processes [1-3]. Therefore, researchers investigated the motion characteristics of single bubble [4-7] and multiple bubbles [7-9].

Pang et al. [6] studied the effect of fluid physical properties on bubble shape, wake characteristic, and terminal velocity in different gravity environment. Balcazar et al. [7] carried out a numerical study on buoyancy-driven motion of single and multiple bubbles, and demonstrated that the new method was numerically stable for a wide range of Morton and Reynolds numbers. Gumulya et al. [9] found that when two bubbles rose in a straight line, the velocity and shape of the trailing bubble were more affected. Yamasaki [10] used a coupled

level-set and volume-of-fluid method to investigate the bubble deformation and explained the mechanism of bubble deformation under presence of given magnetic field.

Kumar et al. [11] utilized volume of fluid (VOF) numerical algorithm to processing the surface tension, transient and steady state bubble deformations, rise velocities, and aspect ratios. Jyeshtharaj et al. [12] found the formation mechanism of waking flow in the bubble column turbulent. Liu et al. [13,14] studied the relationship between the bubble diameter, aspect ratio and bubble terminal velocity. Wu et al. [15] investigated the effects of cross flow velocity and the nozzle radius on the bubble detachment characteristics. The results showed that the bubble frequency and shape at the detachment can be controlled by exerting different cross flow velocities.

The above research mainly focused on the free rising process of bubbles in stationary liquids without the temperature difference. However, the disturbance and heat transfer characteristics of bubbles under different temperatures are not reported. This paper deals with the continuous rise of multi-bubble under the different temperatures. The relevant mathematical model is established to simulate the bubble rising process, and the flow and heat transfer characteristics of bubbles in liquid would be revealed.

2. The establishment of the mode

2.1. Physical model

The calculation area and grid division are shown in Fig.1. The diameter of the calculation region is 0.3 m, and the height is 0.8 m. The upper part is the gas region, with a height of 0.2 m; the lower part is the liquid region, with a height of 0.6 m. The three-dimensional coordinate system is shown in Fig.1, where the coordinate of the center point of the cylindrical bottom surface is (0.15, 0.15, 0) m.

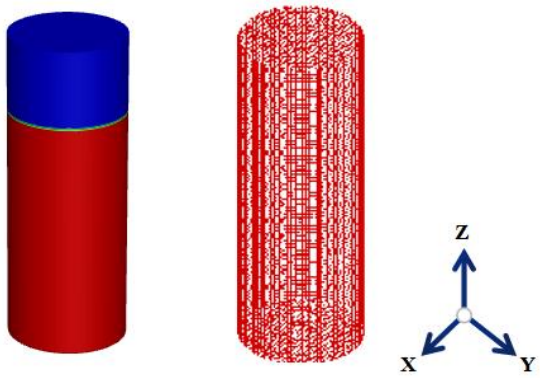

Fig. 1. The schematic diagram of calculation area and grids

Temperature and velocity of the center point of bubble under different grid quantity are shown in Fig.2. As the number of grids exceeds 600,000 grids, the calculating results tend to be stable, which can ensure sufficient accuracy. Because the impact of calculation time and precision should be considered, the grid number is 600,000.

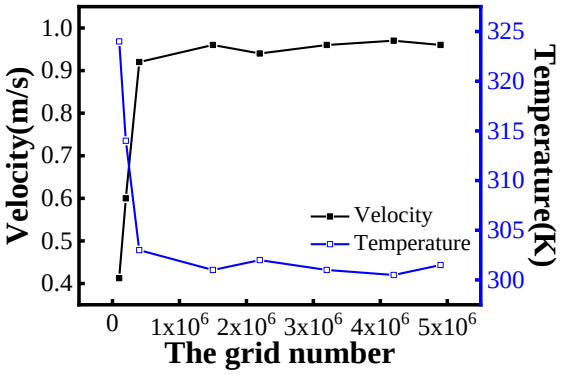

Fig. 2. Mesh generation and independence validation

2.2. Mathematical model

The volume of fluid (VOF) method is used to simulate the volume function α.

$$\frac{\partial \alpha}{\partial t} + \mathbf{u}\nabla\alpha = 0 \tag{1}$$

In the case of two-phase flows, both the μ and the ρ in equation (1) are determined by the volume function α.

$$\rho = \rho_l \alpha + \rho_g (1-\alpha) \tag{2}$$

$$\mu = \mu_l \alpha + \mu_g (1-\alpha) \tag{3}$$

The dynamic viscosity and density of the fluids are μ_l, μ_g, ρ_l and ρ_g respectively, $\boldsymbol{u}$ is the velocity vector.

In VOF method, the gas-liquid interface is tracked by solving the conservation of mass equation of the volume fraction. The conservation of mass equation is given by:

$$\frac{\partial}{\partial t}(\alpha_g \rho_g) + \nabla \cdot (\alpha_g \rho_g v_g) = S_{\alpha_g} + \Sigma_{l=1}^{n}(m_{lg} - m_{gl}) \tag{4}$$

Where, α_q represent the volume fraction of the g phase, ρ_g is the density of the g phase, v_g is the velocity of the g phase, m_{lg} is the mass transfer from the l to the g phase, m_{gl} is the mass transfer from the g to l phase, and S_{α_g} is the source term for the g phase, which is given by

$$\nabla = \frac{\partial}{\partial x} + \frac{\partial}{\partial y} + \frac{\partial}{\partial z}.$$

The velocity field of the two-phase flow model is shown by the phases and is obtained by solving the conservation of mass momentum equation over the entire region. The conservation of momentum equation is given by:

$$\frac{\partial}{\partial t}(\rho v) + \nabla \cdot (\rho v v) = -\nabla \cdot [\mu(\nabla v + \nabla v^T)] + \rho g + F \tag{5}$$

Where, ρ is the fluid density, p is pressure, g is the acceleration of gravity. F is the volume force acting on the control volume. v is the velocity of the fluid. μ is the dynamic viscosity. The temperature field of VOF multiphase flow model is obtained by solving the energy equation in

the whole region.

The energy equation is given by:

$$\frac{\partial(\rho T)}{\partial t}+\nabla\cdot(\rho\cdot\mathbf{u}T)=\nabla\cdot(\frac{k}{c_p}\nabla T)+S \tag{6}$$

T is the temperature of flow field, c_p is the specific heat capacity, k is the thermal conductivity, S is a viscous dissipative term.

The following simplification is made in the calculation processes:

(1) Bubble shapes are considered as spheres.

(2) The wall is adiabatic wall and has no heat exchange with the external environment.

3. Experiment/model validation

3.1. The testing apparatus

The bubble dynamics are characterized by many parameters, such as bubble size, velocity, trajectory and formation mode, and the bubble shape is monitored by imaging technology [13,14].

The schematic diagram of the test system is shown in Fig.3. The reactor is made of plexiglass with a diameter of 0.15 m, and the liquid is water and the height is 0.5 m. The nozzle is u-shaped, which can eliminate the influence of pipe wall on bubble shape. Fluorescein, which can fluoresce in the light of a specific wavelength [18], is added into the liquid. The bubble shape is captured by a high-speed camera with horizontal shooting. After taking comprehensive consideration of the size of the spray gun and the container, the injection depth is set as 0.4m. The initial diameter of the bubble is set around 0.025 m during the test. The initial diameter of the bubble is regulated around 0.025 m by a flow meter.

The continuous laser wavelength is 467 nm. The shooting rate of the high-speed camera is 50 frames per second, with a filter at the camera lens, which can avoid the interference of the natural light and laser.

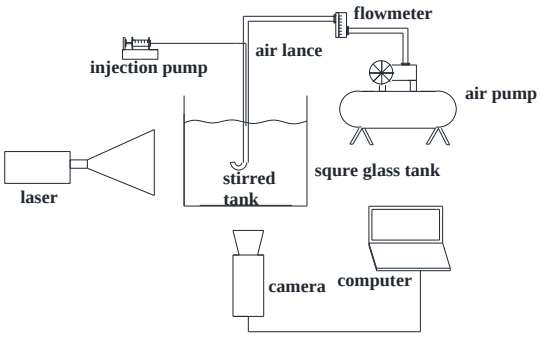

Fig. 3. The schematic diagram of the test system

3.2. Comparison of numerical simulation and test

A continuous bubble model is established with temperature differences. The physical model and grid partition are shown in Fig.1. The center point coordinates of the first bubble and the second bubble are (0.15, 0.15, 0.4) m and (0.15, 0.15, 0.35) m. Experiments are conducted to verify the simulation results, and the results are shown in Fig.4-Fig.6.

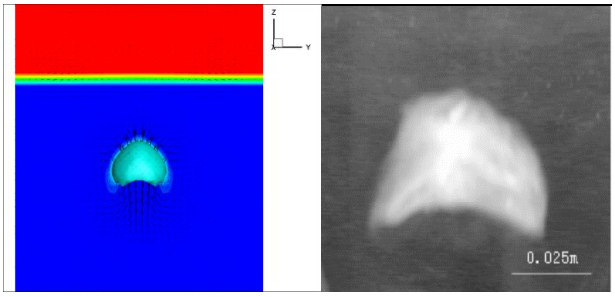

(a) (b)

Fig. 4. A comparison of the (a) simulation results and (b) experimental results of bubble shape at the initial state

As shown in Fig.4, the simulation results are the same with the experimental results. As the bubble rises in the stationary liquid, its shape gradually changes, because of the effects of pressure difference on the upper and lower surfaces. The interval time between the two bubbles when the experiment is carried out is 0.02s, and the test and simulation results of the second bubble shape are shown in Fig.5.

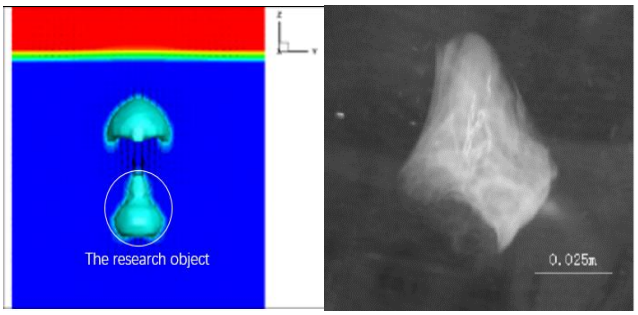

(a) (b)

Fig. 5. A comparison of the (a) simulation results and (b) experimental results of bubble shape at the interval time = 0.02 s

Fig.5 shows that liquid produces annular jet in the process of initial bubble movement. The second bubble is affected by the annular jet produced by the initial bubble, which makes the top part of this bubble is sharp. It can also be observed that the the experimental results are consistent with the simulation results.

As shown in Fig.6, when the interval time is 0.04 s, the bubble shape changed from to the bullet. Because the annular jet in the liquid is mainly distributed around the bubble, when the bubble interval is longer, the greater the distance between bubbles, the stronger influence of annular jet on subsequent bubbles would have. The bubbles are elongated and slightly deformed.

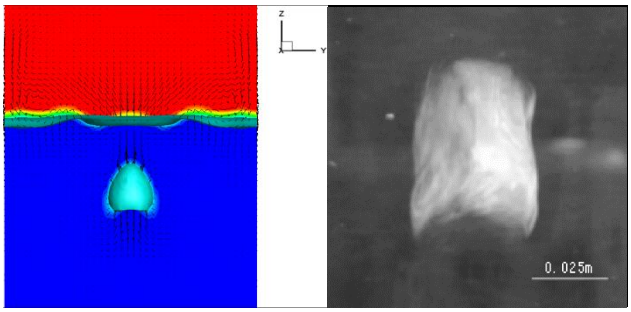

(a) (b)

Fig. 6. A comparison of the (a) simulation results and (b) experimental results of bubble shape at the interval time = 0.04 s

The simulation results in Fig.4 to Fig.6 are consistent with the experimental results, which means that the numerical model is credible. So the following research is based on this model.

4. Flow and heat transfer in continuous bubble rising process

4.1. The aspect ratio of bubbles

The shape and disturbance characteristics of continuous bubbles are investigated. The center positions of the first to fourth bubbles are (0.15,0.15,0.4) m, (0.15,0.15,0.37) m, (0.15,0.15,0.34) m and (0.15,0.15,0.31) m, respectively, the bubble diameter is set as 0.025m, the initial temperature of gas and liquid is 1500 and 300 K.

Table 1 shows the collision time and average velocity, which are the interval time and the average speed for the whole rising process, of continuous bubbles.

Table 1 The collision time and the average velocity.

Bubble number	z(m)	Collision time(s)	Average velocity(m/s)
1	0.4	0.235	0.88
2	0.37	0.21	1.13
3	0.34	0.195	1.25
4	0.31	0.19	1.30

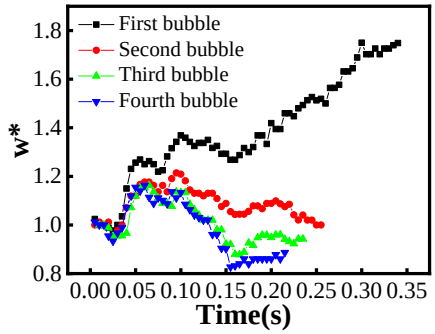

Fig. 7. The variation of w* with time

The aspect ratio (the ratio of width to height, w*) of bubbles is used to demonstrate the degree of bubbles deformation [18,19]. As can be seen in Fig. 7, from the initial time to 0.07 s, w* would first decrease and then gradually increase. The stationary bubble begins to rise and the bubble shape in the initial period is slightly elongated, because of the influence of inertia and resistance. As the bubble rises, because of the influence of pressure difference, the bubble gradually becomes a cap from a ball, which leads to the increase of w*. During the period from 0.07 s to bubble burst, the w* of the first bubble showed a continuously rising trend. The smaller the z value of the bubble, the greater the w* decreases. When the first bubble rises, the liquid is stationary and the bubble is not affected by annular jet. The annular jet has a stretching effect on the rising process, which reduces the w* of the subsequent bubbles. With the continuous occurrence of bubbles, the disturbance effect accumulates, and the jet intensity in the liquid increases. Therefore, the smaller the z value of the bubble, the more obvious the stretching effect is.

4.2. Continuous bubbles velocity

The change of velocity at the bubble center is shown in Fig.8. It can be observed that the velocity first increases and then decreases from the initial time to about 0.07 s. The reason is that the bubble starts to accelerate from static situation under the action of buoyancy.

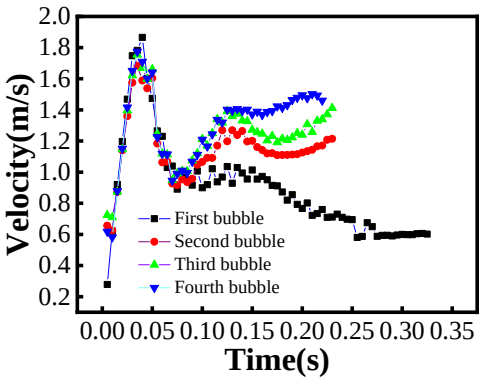

Fig. 8. The velocity of bubble geometry center

As the bubble shape changes, the resistance increases and the velocity decreases. The bubble velocity decreases from 0.07 s to the time when the bubble contacts the free surface. Then the bubble velocity increases slowly. The smaller the z value, the larger the rising velocity is. The first bubble is not affected by the annular jet. As the bubble deforms, the bubble resistance increases and the bubble velocity decreases. Driven by the first bubble annular jet, the subsequent bubble velocity increases. With the continuous disturbance of bubbles, the intensity of annular jet would increase. Therefore, smaller z value would result in greater velocity.

4.3. Continuous bubbles temperature

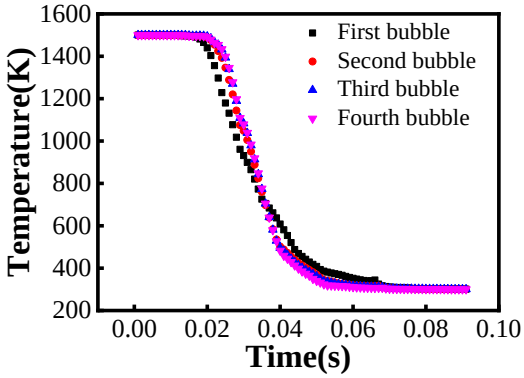

Fig. 9. The variation of bubbles temperature with time

As shown in Fig.9, the bubbles temperature drops rapidly during the rising process of bubble. At 0.08 s, the bubbles temperature drops to about 300 K. The bubble temperature would have more changes in rising process if the bubble carries less heat. In the initial stage, the temperature of the bubble is basically unchanged. As the bubble rises, the temperature of the bubble decreases rapidly. The closer the initial position of the bubble is to the bottom of the cylinder, the slower the temperature drops.The reason is that in the initial stage, the bubble is less affected by the jet, with the rising of the bubble, the jet strength increases, and the closer the bubble is to the bottom of the cylinder, the more affected by the jet, the stronger the heat transfer strength between the bubble and liquid. The later does the bubble generate, the greater strength of the jet would contain by the liquid. The smaller the z value of the bubble, the faster the temperature drops.

5. The influence factors of bubble velocity and temperature

5.1. Bubble diameter

The flow state of liquid will affect the bubbles motion state. In order to investigate the disturbance and heat transfer characteristics of bubbles rising freely in flowing liquid, two continuous bubbles are selected as the research objects. The initial positions of the first bubble and the second bubble are (0.15,0.15,0.4) and (0.15,0.15,0.35) m, respectively. The initial diameter and temperature of the first bubble are 0.025 m and 300 K. The velocity and temperature of the bubble are the velocity and temperature of the central point of the bubble. The second bubble rises freely in the fluid with flowing state, which is induced by the initial bubble's disturbance. The second bubble diameter is set as 0.02 m, 0.025 m, 0.03 m and 0.035 m. The bubbles initial temperature is set as 1500 K, and the disturbance and heat transfer characteristic of the second bubble with different diameter are analyzed.

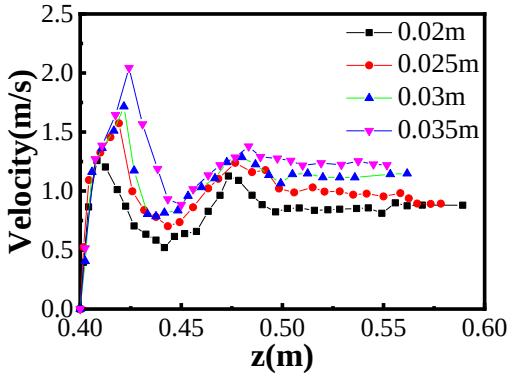

Fig. 10. The variation of the second bubble velocity with z

Fig. 10 shows the velocity of the second bubble. The bubble velocity first increases, then decreases, then increases slowly, and finally tends to be stable. At the same height, the bubble velocity increases with the increase of bubble diameter, because the buoyancy increases with the increase of bubble diameter. The greater the buoyancy, the faster the bubble rises. At the height of 0.45 to 0.48 m, the bubble velocity rises slowly under the influence of jet flow. Smaller bubble diameter would result in greater changes in bubble velocity. The decrease of the bubble diameter would have obvious effects, because the inertial force of the bubble would be smaller, the annular jet would have more effects on the bubble, and the influence of the liquid jet on the small diameter bubble would be greater.

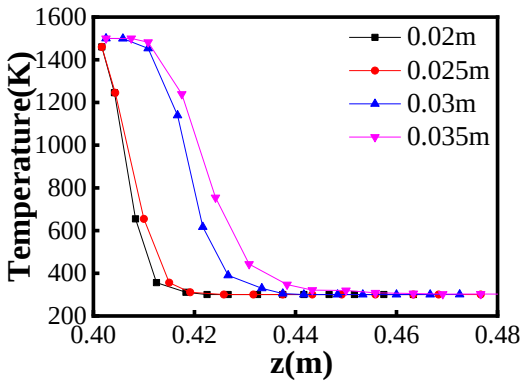

Fig. 11. The variation of the second bubble temperature with z

The temperature of the second bubble is shown in Fig.11. The bubble temperature drops to about 300 K in a short time. At the same height, as the bubble diameter increases, the bubble temperature rises. The larger diameter improves the heat carrying capacity and heat transfer intensity of the bubbles.

5.2. Surface tension

The initial bubble parameter is set the same with section 5.1, the second bubble parameter is 0.025 m. The high-temperature bubbles with surface tension of 0.18 N/m, 0.2 N/m, 0.22 N/m, 0.24 N/m and temperature of 1500 K are generated at (0.15, 0.15, 0.4) m. The disturbance and heat transfer of high temperature bubbles under different surface tension in the same liquid jet condition are analyzed.

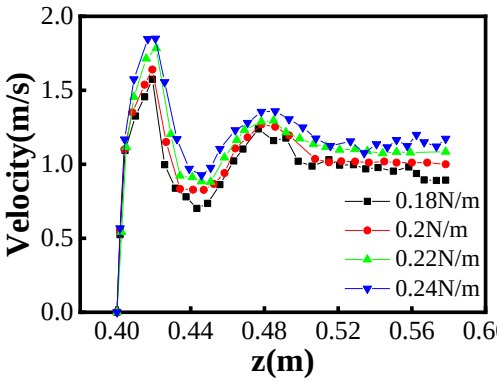

Fig. 12. The variation of the second bubble velocity with z

As shown in Fig. 12, at the same height, larger surface tension would result in larger bubble velocity. Larger surface tension enhances the ability of the bubble to maintain its shape. When the bubble rises from 0.44 to 0.46 m, the bubble rises slowly under the influence of annular jet. With the increase of surface tension, the bubble velocity changes slower, the bubble shape variable is smaller, the bubble is closer to the sphere, and the less resistance the bubble has.

6. Conclusion

The rising process and temperature of bubbles are studied by VOF method and compared with experimental results for verification. Several conclusions can be drawn as follows:

(1) In the continuous bubbles rising process, the annular jet generated by the bubble, which disturbance the liquid, will stretch the subsequent bubbles. The annular jet also reduces the w*, improves the bubble velocity, reduces the disturbance effect of bubble on liquid, and strengthens the heat transfer intensity of bubble.

(2) When the liquid is in the flow state, the movement of small bubbles shows more obvious changes, and the large bubbles have larger heat transfer intensity. The smaller the bubble surface tension is, the greater the change of bubble flow state is.

Acknowledgement

The authors graciously acknowledge the financial support provided by Science Research Foundation of Yunnan Education Department (NO. 2019J0033) and the National Natural Science Foundation of China (NO. 51966005).

Nomenclature

t	Time (s)	Greek symbols	
p	Pressure (Pa)	α	Volume fraction
g	Gravitational acceleration (m/s^2)	ρ	Density (kg/m^3)
w*	Ratio of bubble width to height	μ	Viscosity (Pa×s)

T	Temperature (K)	σ	Surface tension (N/m)
U	Velocity vector (m/s)	*v*	Velocity (m/s)
c_p	Specific heat capacity (J/K)	Subscripts	
x,y,z	Cartesian coordinate (m)	*g, l*	Gas, liquid Phase

References

[1] Darton, R. C., Bubble-growth Due to Coalescence in Fluidized-beds, *Trans inst chem.eng., 55* (1977), 4, pp. 274-280.

[2] Chernika, I. M., *et. al.*, Heat Transfer Features under Bubble Boiling in an Electroconvection Flow, *Surface Engineering and Applied Electrochemistry, 56* (2020), 2, pp. 208-215.

[3] Qi, B., et. al., Influences of Wake-effects on Bubble Dynamics by Utilizing Micro-pin-finned Surfaces under Microgravity, *Appl. Therm. Eng.,113* (2017), pp. 1332-1344.

[4] Zhang, Y., *et. al.*, Numerical Study of Bubble Rising Motion in a Vertical Wedge-Shaped Channel Based on a Modified Level Set Method, *Fluid Dyn., 55* (2020), 2, pp. 241-251.

[5] Zhou, Y., *et. al.*, Analyses and Modified Models for Bubble Shape and Drag Coefficient Covering a Wide Range of Working Conditions, *Int. J. Multiph. Flow., 127* (2020), pp. 103265.

[6] Pang M., *et. al.*, Numerical Study on Dynamics of Single Bubble Rising in Shear-thinning Power-law Fluid in Different Gravity Environment, *Vacuum., 153* (2018), pp. 101-111.

[7] Balcázar N., *et. al.*, Level-set Simulations of Buoyancy-driven Motion of Single and Multiple Bubbles, *Int. J. Heat Fluid Flow, 56* (2015), pp. 91–107.

[8] Zhang, S., *et. al.*, Simulation of Air Gun Bubble Motion in the Presence of Air Gun Body Based on the Finite Volume Method, *Appl. Ocean Res., 97* (2020), pp. 102095.

[9] Gumulya, M., *et. al.*, Interaction of Bubbles Rising Inline in Quiescent Liquid, *Chem. Eng.Sci., 166* (2017), 3, pp. 1–10.

[10] Yamasaki, H., *et. al.*, Numerical Simulation of Bubble Deformation in Magnetic Fluids by Finite Volume Method, *J. Magn. Magn. Mater., 431* (2017), pp.164-168.

[11] Kumar, P., *et. al.*, Effects of Confinement on Bubble Dynamics in a Qquare Duct, *Int. J. Multiph. Flow., 77* (2015), pp. 32–47.

[12] Jyeshtharaj, B. *et. al.*, Bubble Generated Turbulence and Direct Numerical Simulations, *Chem. Eng. Sci., 157* (2017), pp. 26–75.

[13] Liu, L., *et. al.*, Experimental studies on the shape and motion of air bubbles in viscous liquids, *Exp. Therm Fluid Sci., 62* (2015), pp. 109-121.

[14] Liu, L., *et. al.*, Experimental Studies on the Terminal Velocity of Air Bubbles in Water and Glycerol Aqueous Solution, *Exp. Therm Fluid Sci., 78* (2016), pp. 254-265.

[15] Wu, W., *et. al.*, Numerical Investigation of 3D Bubble Growth and Detachment, *Ocean Eng., 138* (2017), pp. 86-104.

[16] Zhang, A., *et. al.*, An SPH Modeling of Bubble Rising and Coalescing in Three Dimensions, *Comput. Meth. Appl. Mech. Eng., 294* (2015), pp. 189-209.

[17] Rahmat, N. *et. al.*, The Combined Effect of Electric Forces and Confinement Ratio on the Bubble Rising, *Int. J. Heat Fluid Flow., 65* (2017), pp. 352-362.

[18] McClure, D. D, *et. al.*, Mixing in Bubble Column Reactors: Experimental Study and CFD Modeling. *Chem Eng J, 264* (2015), pp. 291–301.

[19] Legendre, D., *et. al*., On the Deformation of Gas Bubbles in Liquids. *Phys. Fluids., 24* (2012), 4.

- Paper submitted: 15 February 2021
- Paper revised 17 June 2021
- Paper accepted: 23 June 2021